JOURNAL OF MATERIALS SCIENCE **39** (2004) 5719–5726

Morphologies and properties of nickel particles prepared by spray pyrolysis

DONG-JUN KANG, SUN-GEON KIM
Department of Chemical Engineering, Chung Ang University, 221, Huksuk-Dong, Dongjak-Ku, Seoul 156-756, Korea
E-mail: sgkim@cau.ac.kr

HYUN-SUK KIM
Sunjin Chemical Co. Ltd., 836-1 Wonsi-Dong, Ansan, Kyungki-Do 425-852, Korea

Nickel particles were prepared by spray pyrolysis of aqueous solutions of $NiCl_2 \cdot 6H_2O$ with reducing gas. Wet pyrolysis lowered the onset and the finishing temperatures of the individual chemical transformations by at least 100°C to contribute high conversion to nickel and its completion of sintering. Densification by increasing the furnace set temperature outweighed the adverse effects of the dry sintering and short residence time of the precursor particles. The initial salt concentration increased the size of the nickel particles with their densification, resulting from the enhanced rate of nickel nucleation.

1. Introduction

Nickel particles have been replacing palladium particles as electrode materials for multilayer ceramic chip (MLCC) due to their low cost [1]. Recently nickel-based MLCC even achieved better performances than palladium-based one in migration, reliability, capacitance values, insulation resistance, breakdown voltage and resistivity [2]. In order to obtain such performances, the nickel particles should be spherical and highly crystalline with smooth surfaces. Spray pyrolysis has been one of the excellent candidates for this purpose. The morphology of the nickel particles is highly dependent on the condition of spray pyrolysis as well as the nature of nickel precursors [3–5]. However, few systematic studies to characterize this dependency have been found. Nagashima *et al*. [6] prepared the nickel particles by spray pyrolysis of $Ni(NO_3)_2 \cdot 6H_2O$ aqueous solution with 20 vol% H_2 in N_2. Hollow particles with rough surfaces were obtained at 700 to 900°C while the particles became solid and spherical with smooth surfaces up to 1500°C. On the other hand Stovic *et al*. [7] prepared, from $NiCl_2 \cdot 6H_2O$ with 20 vol% H_2 in N_2 between 700 and 900°C, relatively spherical nickel particles. They discussed the morphology according to the residence time of the precursor in the reactor. Che *et al*. [8] obtained dense nickel particles from $Ni(NO_3)_2 \cdot 6H_2O$ aqueous solution by spray pyrolysis with 15 vol% H_2 in N_2. Hollow nickel oxide particles with rough surfaces formed at low temperature reduced to hollow nickel particles by H_2 above 300°C. Subsequent intraparticle sintering of nickel crystallites yielded the densification of the nickel particles as the temperature increased. In a previous study [9], we discussed the morphology of nickel oxide particles, the intermediates to nickel particles, by spray pyrolysis of the aqueous solution of $NiCl_2 \cdot 6H_2O$ with argon only. We showed the effects of the elementary processes, such as the drying of salt droplets, decomposition of crystalline water, precipitation of salt and oxidation of the salt, empathizing the roles of salt solubility in its precipitation and volume reduction in the salt to oxide transformation.

In this study we have proceeded to the nickel particles by reductive spray pyrolysis of $NiCl_2 \cdot 6H_2O$ solution. Their morphologies and properties have been investigated by inserting preliminary drying, and varying the furnace set temperature and initial salt concentration.

2. Experimentals

The apparatus for preparation of nickel particles by spray pyrolysis consisted of ultrasonic nebulizer, diffusion dryer, tubular reactor in electrical furnace, filter and acid gas absorber, as shown in Fig. 1. An aqueous solution of $NiCl_2 \cdot 6H_2O$ solution with various concentrations (reference concentration was 0.5 M) maintained at 30°C was nebulized indirectly at a rate of 15 ml/h. The droplets were carried by either argon gas (99.99%) at 2.5 l/min or 10%H_2–90% argon in volume at 1.25 l/min to an electrically heated (reference furnace set temperature was 900°C) tubular reactor 800 mm long with the diameter of 32 mm. In the former, the mixture gas containing 10%H_2–90% argon was introduced at 1.25 l/min to the annular space of a concentric tubular reactor so that the droplets and hydrogen could be heated separately before they met. This configuration was abbreviated as TT, hereafter which meant *t*hermally dried droplets with hydrogen introduced in *t*ubular reactor. On the other hand, in case of the latter, the balance argon gas at 2.5 l/min was introduced to the same place, abbreviated as TF, where F means hydrogen introduced

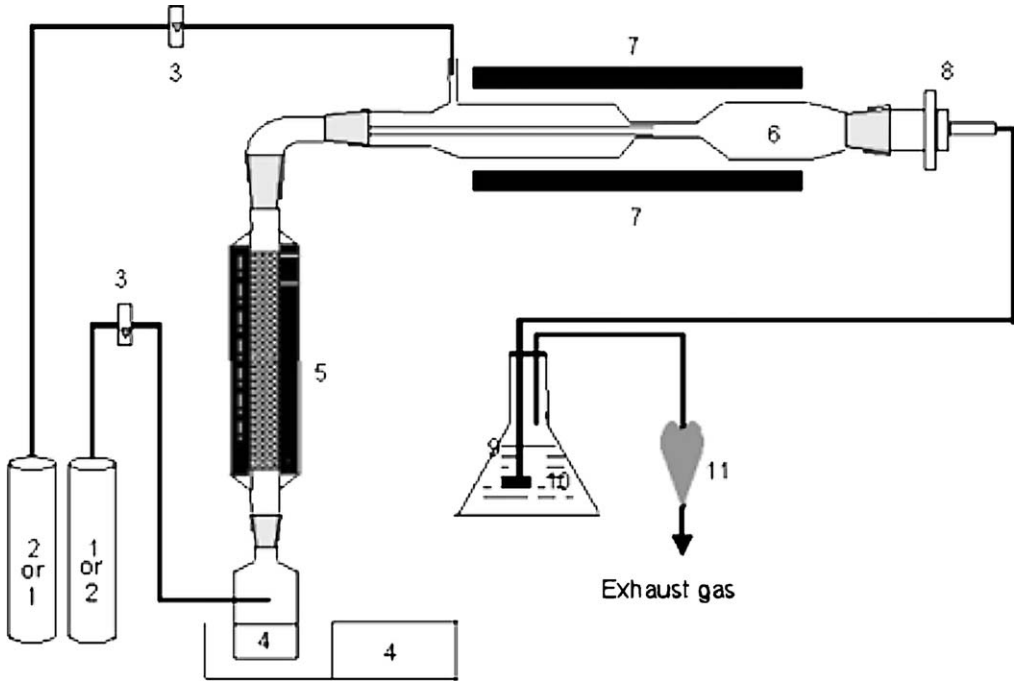

Figure 1 Schematic diagram of overall experimental apparatus. 1. Ar Gas; 2. H_2 Gas; 3. Flow meter; 4. Nickel salt solution; 5. Ultrasonic nebulizer; 6. Reactor; 7. Electrical Furnace; 8. Filter; 9. Bubbler; 10. NaOH solution; 11. Hydrogen burner.

to nebulizing flask. The droplets passed diffusion dryer with the dimension described elsewhere [9], if necessary, in order to see the effect of preliminary drying, in which case "D" preceded the abbreviations such as DTT and DTF. Thus we have four configurations such as TT, TF, DTT and DTF, as shown in Table I. In the middle of the furnace, the two streams from inner tube and annular space met in the neck with decreased cross section to enhance their mixing.

In addition to the reactor configurations, the process variables included the initial concentration of the nickel salt and furnace set temperature in order to investigate their effect on the size, morphology, crystallinity and chemical nature of the product particles. The particles exiting from the reactor were collected by filtration. The water vapor and acid formed was finally absorbed in caustic solution before exhausting the waste gas. The particles collected were characterized in the same manner described elsewhere [9].

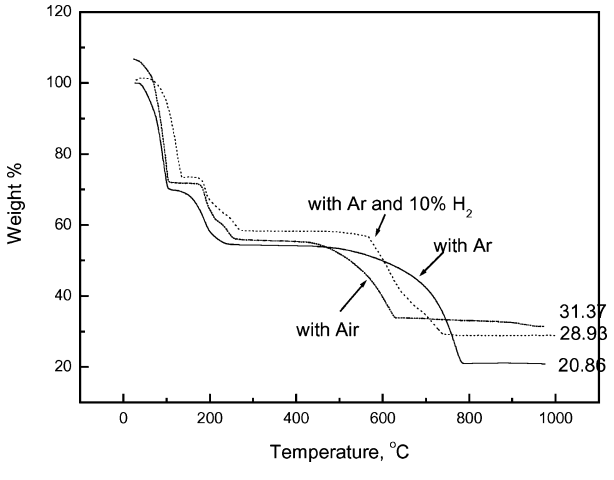

Figure 2 Thermogravimetric analyses of $NiCl_2 \cdot 6H_2O$ under various gas conditions. (Heating rate: 20°C/min).

3. Results and discussion

3.1. Thermogravimetric analyses of nickel salts

Fig. 2 shows thermogravimetric analyses of the reagent $NiCl_2 \cdot 6H_2O$ with argon, air, and 10%H_2–90% argon mixture. Weight losses in all the samples were initiated by removal of crystalline water: six molecules of crystalline water were removed stepwise, first four out of six and then the remaining two, which completed up to 280°C. Above the temperature the weight loss stopped until chemical transformation such as either oxidation or reduction of the dehydrated salt took place, depending on the gas environment. With air, the dehydrated salt began to oxidize at 420°C and the oxidation ceased

TABLE I Abbreviation of reactor configuration

	TT	TF	DTT	DTF
Types of drying	Thermal drying only	Thermal drying only	Diffusion and thermal frying	Diffusion and thermal drying
Position of hydrogen introduced	Tube in furnace	Spraying flask	Tube in furnace	Spraying flask

at 620°C, while with hydrogen the salt directly reduced between 570 and 730°C. In the argon environment the final weight loss occurred with wider temperature range between 420 and 790°C to result in the highest loss among the three. The onset temperature of the weight loss in the argon was the same as that in the air while its finishing temperature was higher than that in the hydrogen environment. Thus it is supposed that the mechanism of beginning the weight loss would be the same in both the air and the argon, which would be decomposition of the dehydrated salt. In the air environment, the salt decomposed in turn transformed to the oxide by the reaction with oxygen. On the other hand in the argon the salt kept on decomposing to metallic nickel. Since the rate of the decomposition was probably lower than that of the direct reduction by hydrogen, the former would end at higher temperature than the latter, as described before. In the case of argon, though major weight loss came from the reductive decomposition of the salt, compared to the curves for air and hydrogen environments, the additional weight loss would be contributed by sublimation of the salt. The reason for this is that the dehydrated salt had a chance to sublime before the decomposition took place in such wider range of temperature [9]. In the real situation, in addition to the salt and hydrogen, there coexists water coming from decomposition of crystalline water in the salt as well as evaporation of the droplets. The water was believed to take part in the oxidation of the salt instead of oxygen, forming intermediate oxide, which was then reduced by hydrogen to final nickel [8].

3.2. Effect of reactor configurations

Four modes of reactor configuration were used as TT, DTT, TF and DTF, as described before. In general, TT particles resembled DTT as TF did DTF, which implied that the insertion of the diffusion dryer did not

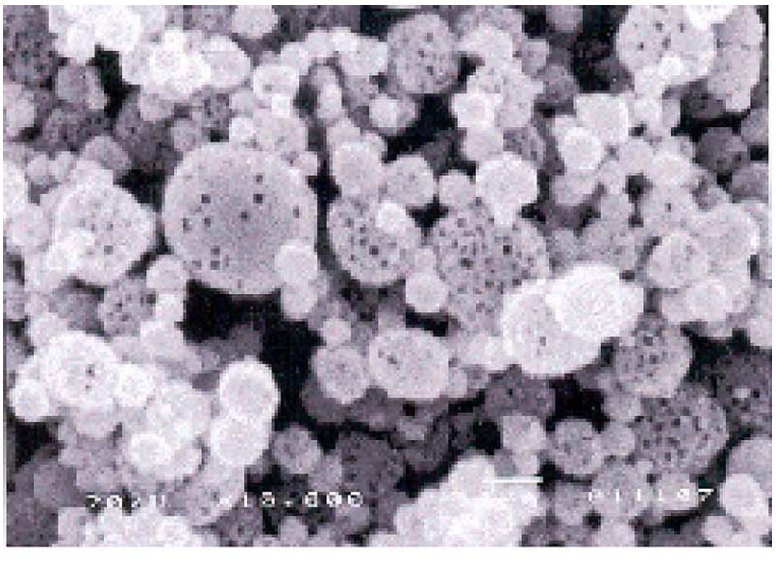

(a)

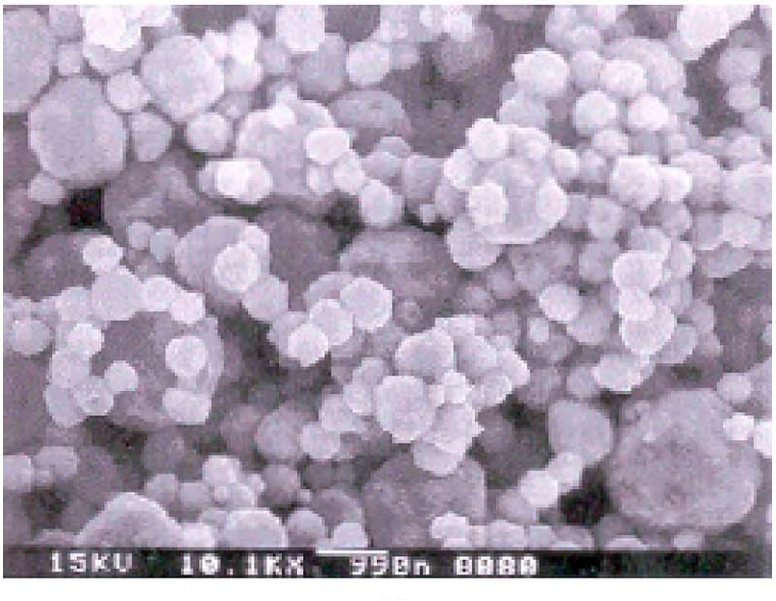

(b)

Figure 3 SEM pictures of (a) DTT and (b) TF nickel particles prepared, otherwise under reference condition.

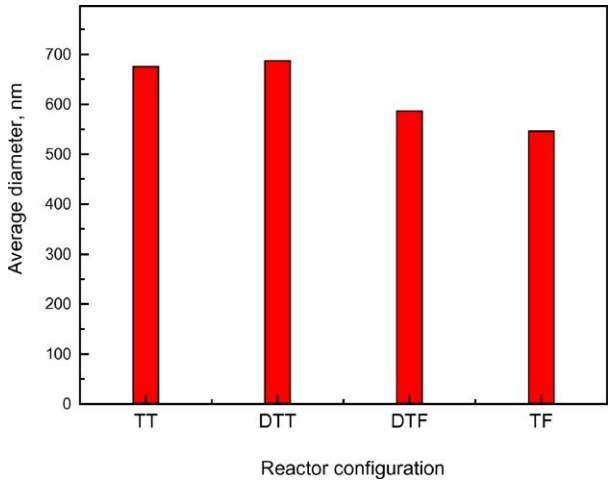

Figure 4 Comparison of diameters of DTT, TT, DTF, and TF particles prepared under reference condition.

decisively influence the morphology of the nickel particles. This was not the case for the nickel oxide [9], where the preliminary drying significantly affected the hollowness as well as the size of the particles. Fig. 3 shows SEM images of DTT and TF particles prepared under the reference conditions. The former were relatively large and spherical with some honeycomb-like appearance while the latter were small and relatively far from spherical with internal solidness. Fig. 4 shows the average diameters of the particles prepared under reference conditions by the different modes of reactor configuration. Each diameter was obtained by averaging the number mean diameters of six samples prepared for each corresponding configuration and the error in each bar was within 6%. The standard deviations of the particle diameters in each sample were about 1.4. DTT particles were the largest, followed by TT, DTF and TF in the order of decreasing size. For the port of hydrogen introduction fixed, the preliminary drying increased the average diameter of the particles, even though not so significant as the oxide particles. As described in our previous study [9], the salt particles resulted in relatively solid particles when preliminary drying was inserted, whose size changed little during oxidation. Otherwise, the salt particles became hollow, which shrink by collapse due to oxidative densification. Thus such effect of the diffusion dryer still remained in the final nickel particles: DTT and DTF particles were larger than TT and TF, respectively. Under reference condition the XRD patterns of the particles were all nickel without any traces of chloride and oxide, irrespective of the modes of reactor configuration. In the case in which hydrogen was directly introduced into the

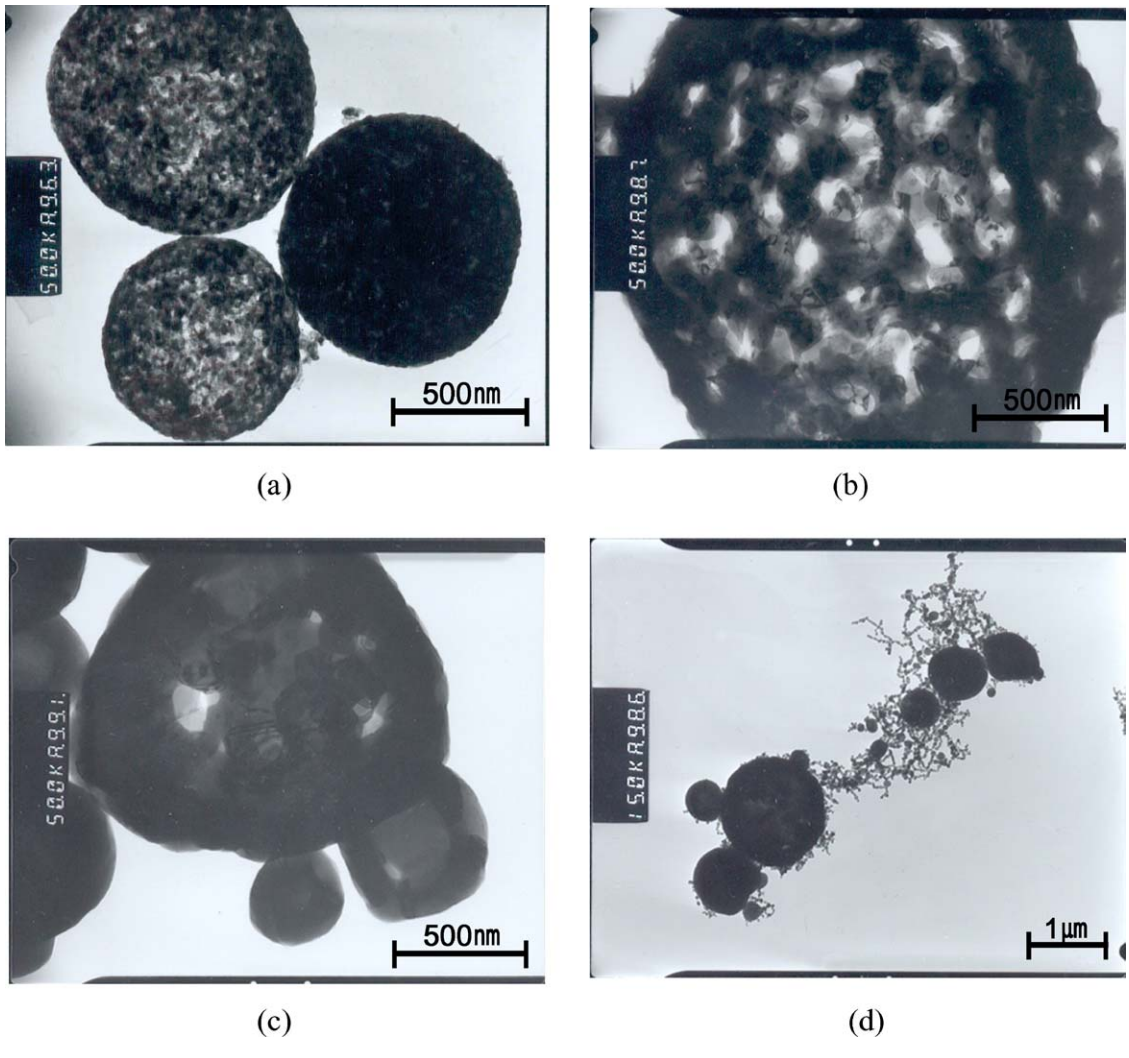

Figure 5 Comparison of (a) nickel oxide, (b) honeycomb-like TT and (c) sintered TF (d) nanosized nickel particles occasionally found in TF under reference condition.

reactor tube such as in DTT and TT, the droplets, before they met the hydrogen, would form oxide particles [9]. As described elsewhere [9], single oxide particle was composed of very small oxide nuclei generated from the salt, which remained without sintering due to their high sintering onset temperature(about 1300°C [8]). When the oxide particles met hydrogen at the mixing junction, they completely transformed to metallic nickel particles under the reference condition, as already discussed with XRD patterns. Even after the complete chemical reduction to nickel, initial single nickel particle would be composed of many tiny nickel crystallites directly converted from the oxide nuclei. Since the onset sintering temperature of nickel nanoparticles is somewhere between 200 and 300°C [8], the nickel crystallites would easily undergo intraparticle sintering forming initially dumbbell-like aggregates, whose three dimensional appearance would be honeycomb-like, and finally single solid nickel particles as completely sintered forms. Many TT and DTT particles were found honeycomb-like since in those modes there was insufficient residence time for complete sintering. On the contrary, when hydrogen was introduced to the nebulizer as in the configurations of TF and DTF, sufficient residence time would be given for the subsequent intraparticle sintering. Thus TF and DTF particles became smaller, more solid and less spherical compared to their counterparts. In addition, as will be described later, TF and DTF modes enhanced the overlap of the oxidation and the reduction to increase the rate of the latter. This not only prolonged the time for sintering but also increased the rate of nickel nucleation, as will be also discussed later, all of which further enhanced the rate of sintering to contribute such morphology of the particles. The sequence from oxide to sintered nickel particles is shown in Fig. 5 by TEM images

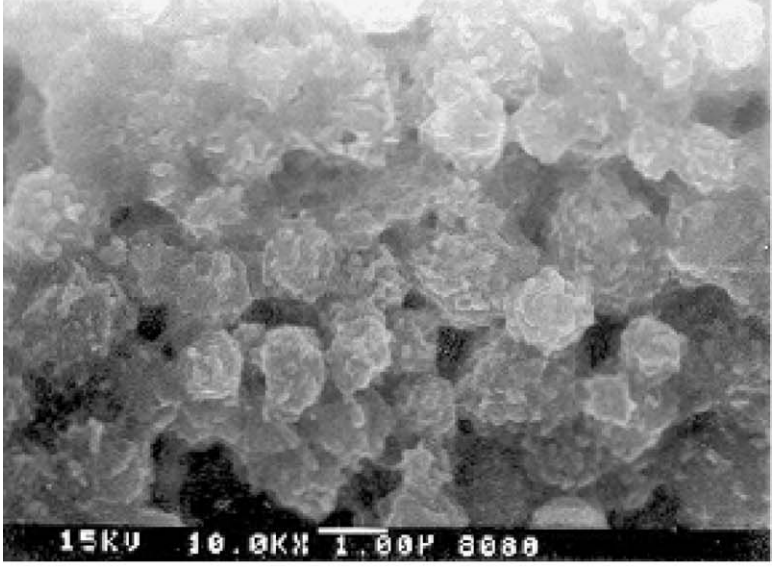

(a)

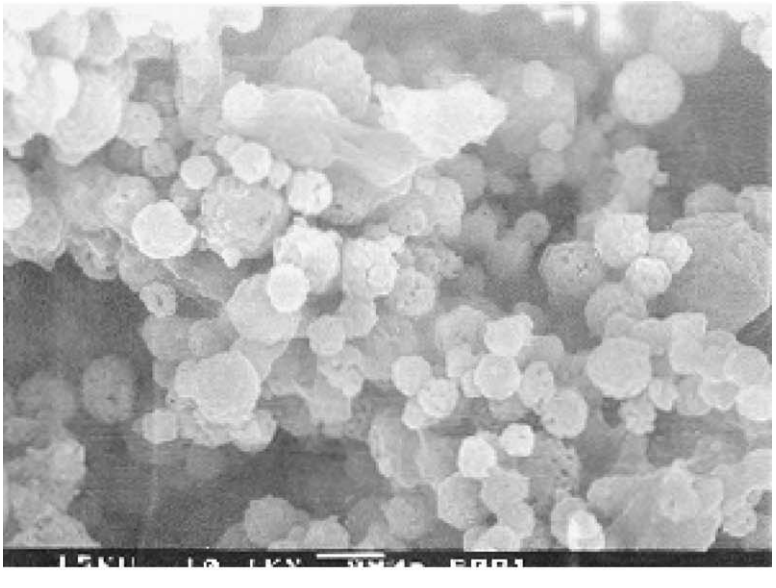

(b)

Figure 6 SEM pictures of TF-nickel particles prepared at various furnace set temperatures, otherwise under reference condition: (a) 300°C, (b) 500°C, (c) 750°C, and (d) 1050°C. *Continued*

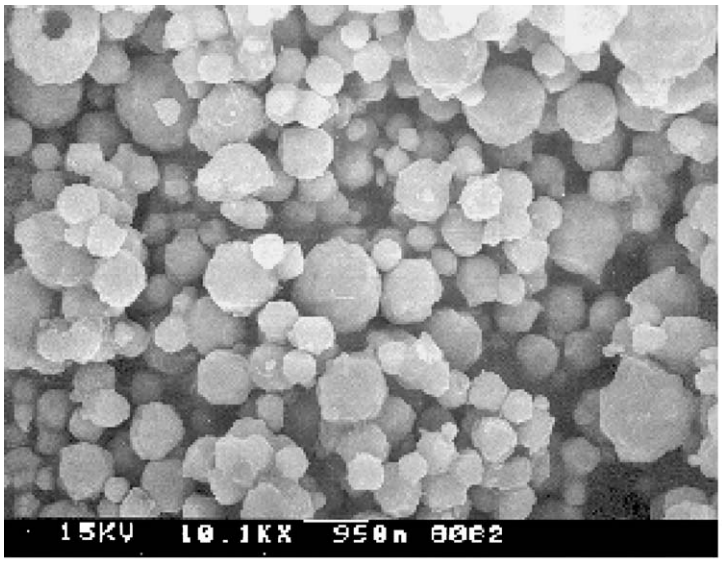

(c)

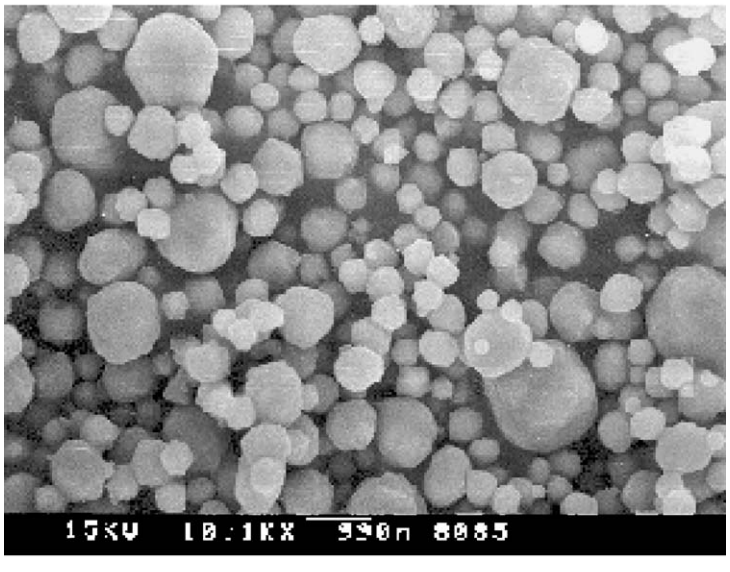

(d)

Figure 6 (Continued).

of the particles of oxide, and nickel during and after sintering.

Aside from the discussion of the effect of reactor configuration, nanoparticles were sometimes observed as shown in Fig. 5d, irrespective of the configuration modes, but the general condition where they appear have not be found yet. They were probably formed from vapor-to-solid conversion starting from salt vapor sublimed, as discussed before.

3.3. Effect of temperature

Figs 6 and 7 show SEM images and XRD patterns of TF particles prepared at different furnace set temperatures, respectively. The usual particulate form was not observed until the honeycomb-like particles appeared at 500°C. From the XRD patterns of the samples, first nickel oxide and metallic nickel appeared at 300 and 500°C, respectively, with traces of the chloride. As the

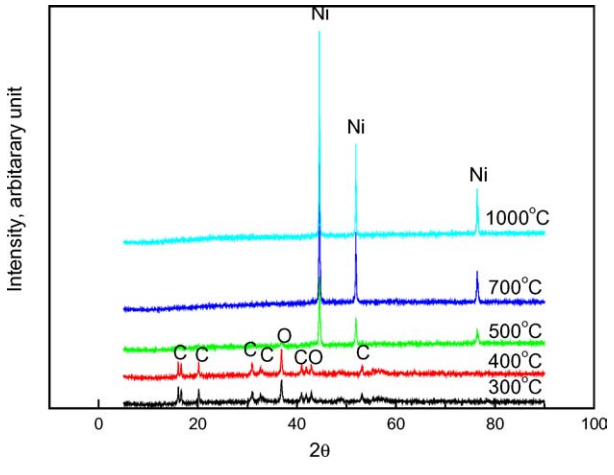

Figure 7 XRD patterns of TF particles prepared from $NiCl_2 \cdot 6H_2O$ at various furnace set temperatures. (C represents for chloride and O for nickel oxide.)

temperature increased, the particles became solid and small with the disappearance of the honeycomb as well as the decrease in surface roughness. All the chloride and oxide peaks disappeared around 600°C, indicating completion of the final reduction, and the crystallinity of the nickel particles then increased with the temperature. In the previous study [9] on the oxide particles prepared with argon only, traces of chloride were left even up to 1000°C. From this it is supposed that the rate of reduction was high enough and thus the rate of oxidation controlled that of overall chemical transformation. Therefore, with hydrogen the intermediate oxide was rapidly consumed, which completed the oxidation of the chloride at a temperature lower by at least 400°C than without hydrogen. On the other hand, in real spray pyrolysis, as shown in Fig. 7, the onset temperatures of both the oxidation and reduction as well as the finishing temperature of the reduction were all lowered by more than 100°C than the corresponding temperatures in the thermogravimetric analyses shown in Fig. 2. Then, the removal of crystalline water, the oxidation of the salt and the reduction of the oxide would take place consecutively with significant overlap between them. It is thus apparent that the water left in the particles would accelerate the rates of the latter two chemical transformations. However, for TT particles, the nickel peaks were not found until 600°C at which the chloride and oxide peaks still remained (not shown). In the mode, since hydrogen was not met until the mixing junction, the reduction had little chance of overlap with the oxidation as well as the removal of crystalline water. There were thus two reasons why the reduction was retarded in the TT mode: one was that the water was not left in the oxide particles and the other was that time was not sufficient for their reduction.

Fig. 8 shows the variation in average diameter of DTT and TF particles with respect to furnace set temperature, otherwise under reference condition. The size of the particles decreased with the temperature, independent of the reactor configurations. The DTT particles are larger than the TF at the given temperature.

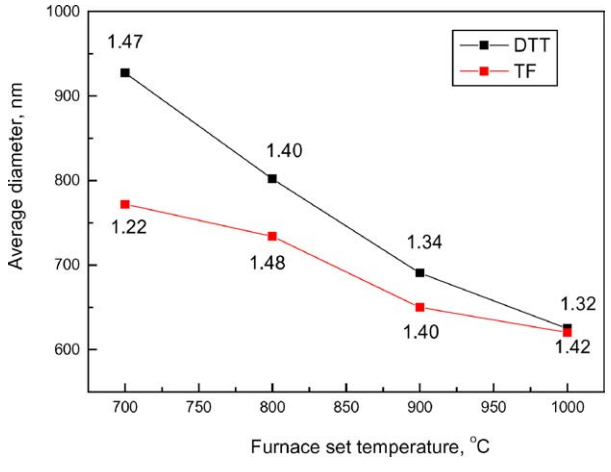

Figure 8 Average diameters of DTT and TF particles prepared from $NiCl_2 \cdot 6H_2O$ with respect to furnace set temperatures, otherwise under reference condition.

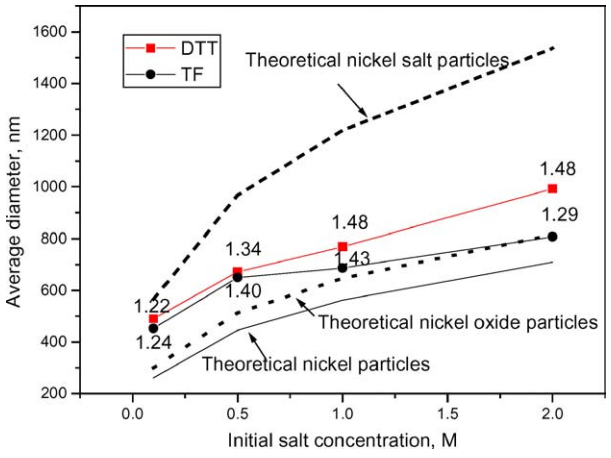

Figure 9 Diameters of DTT, TT and TF particles prepared from $NiCl_2 \cdot 6H_2O$ with respect to initial salt concentrations.

The size difference in the two configurations decreased with the temperature to zero at 1000°C, due to the effect of sintering. Again this was not the case for the oxide particles, as discussed elsewhere [9].

3.4. Effect of initial salt concentration

The morphology of the particles were apparently unchanged by the increase in the initial salt concentration except their size. Fig. 9 shows the effect of the initial salt concentration on the average diameter of DTT and TF particles prepared. Based on the initial droplet diameter of 3 μm, the diameters of theoretically dense particles of salt, oxide and metallic nickel calculated [6, 9] are also shown in the Figure. Since the densities of the salt, oxide and metallic nickel were 3.544, 7.65 and 8.9, respectively [10], the size of the dense particles decreases in that order. Again the DTT particles were larger than the TF particles. All the nickel particles prepared were larger than the dense nickel particles and even dense nickel oxide particles. The sizes of all the particles, irrespective of the reactor configuration, increased with the concentration, as expected. However, the difference in the sizes of the true and the theoretically dense nickel particles decreased with the concentration. If the particles had had the same degree of densification with respect to the initial salt concentration, the plot of their size vs. the initial concentration would have located in the same relative position with respect to the plots for the dense particles as in the case of the oxide particles [9]. On the other hand, the peak heights in the XRD patterns of the nickel particles increased substantially with the initial salt concentration reaching 95% of those of reagent nickel at 2 M, as shown in Fig. 10. It is highly probable that the densification of the nickel particles with the concentration shown in Fig. 9 was related to the increase in the crystallinity. The rate of nucleation increased with the initial salt concentration This decreased the size of nuclei but increased their number substantially [11], which caused such nuclei to get the increased chance of crystalline growth accompanying the densification of the particles.

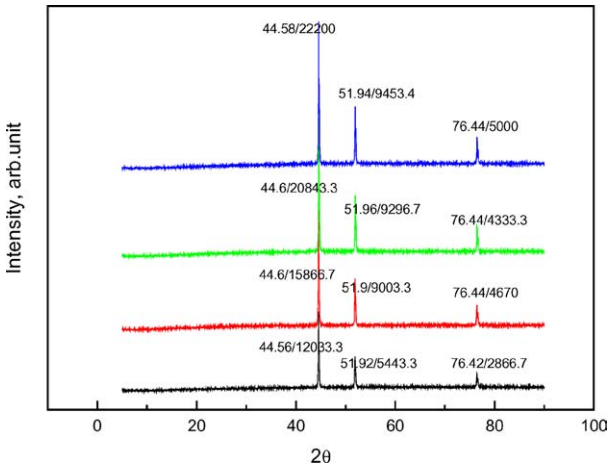

Figure 10 XRD patterns of nickel particles prepared at different initial salt concentrations, otherwise under reference condition.

4. Conclusions

Nickel particles were prepared by spray pyrolysis of aqueous solutions of nickel chloride with 10 vol%H_2–90 vol% argon mixture. Existence of water in the wet chemical transformation occurred in the spray pyrolysis apparently enhanced their oxidation and the subsequent reduction of the oxide particles by lowering their onset and finishing temperatures by more than 100°C. In spite of the low onset sintering temperature of nickel, the particles were observed in honeycomb-like structure during their sintering. These particles were found with high probability in case that their residence time was short for the completion of the sintering and the water was intentionally removed before the reduction of the oxide particles. More densification took place with the furnace set temperature by reducing the size of the particles. The promoted sintering with the temperature outweighed the short residence time and the lowered rate caused by the dry reduction. The initial salt concentration increased the size of the nickel particles with some densification due to the enhancement of rate of crystalline growth.

Acknowledgement

This Research was supported by the Chung-Ang University Special Research Grants in 2003.

References

1. T. ADDONA, P. AUGER, C. CELIK and G. CHEN, *Pass. Comp. Ind.* **Nov./Dec**. (1999) 14.
2. M. TANAHASHI, http://www.reed-electronics.com/ecnmag/ index.asp?layout=article&articleid=CA43450 (2000).
3. B. XIA, I. W. LENGGORO and K. OKUYAMA, *J. Mater. Res.* **15** (2000) 2157.
4. *Idem.*, *J. Amer Ceram. Soc.* **84** (2001) 1425.
5. J. H. KIM, T. A. GERMER, V. I. BABUSHOK, G. M. MULHOLLAND and S. H. EHRMAN, *J. Mater. Res.* **18** (2003) 1614.
6. K. NAGASHIMA, M. WADA and A. KATO, *ibid.* **5** (1990) 2828.
7. S. STOVIC, I. ILIC and D. USKOKOVIC, *Mater. Lett.* **24** (1995) 369.
8. S. L. CHE, K. TAKADA, K. TAKASHIMA, O. SAKURAI, K. SHINOZAKI and N. MIZUTANI, *J. Mater. Sci.* **34** (1999) 1313.
9. D. J. KANG, H. S. KIM and S. G. KIM, *ibid.* Submitted (2003).
10. R. H. PERRY and D. W. GREEN, "Perry's Chemical Engineer's Handbook," 7th ed. (McGraw-Hill, 1997).
11. J. R. BROCK, "Aerosol Microphysics I," edited by W. H. Marlow (Springer-Verlag, Heidelberg, 1980).

Received 12 August 2003
and accepted 11 May 2004